20

Spectral manifestations of carboxylated nanodiamonds complexation with glycine

© P.A. Zhulidin[1], I.L. Plastun[1], P.D. Filin[1], P.Yu. Yakovlev[2]

[1] Gagarin Saratov State Technical University,
410054 Saratov, Russia
[2] RTA Research Center LLC,
117292 Moscow, Russia

e-mail: zhulidin@mail.ru

Received December 28, 2023
Revised January 29, 2024
Accepted March 05, 2024

An analysis of glycine with carboxylated nanodiamonds two-component mixture IR spectra is presented. The study includes interpretation of absorption bands maxima responsible for hydrogen bonding between the main functional groups of glycine and nanodiamond. IR spectra were calculated using the density functional theory (DFT) method using the B3LYP functional. Experimental IR spectra were measured using an IR spectrometer with Fourier transform IR200 Thermo nicolet. Identification of glycine and carboxylated nanodiamonds intermolecular interaction features, manifested in the form of changes in IR spectra, will be important for targeted drug delivery methods modernization, such as glycine, using modified nanodiamonds as carriers.

Keywords: glycine, nanodiamonds, IR spectrum, density functional theory, hydrogen bonds.

DOI: 10.61011/EOS.2024.03.58749.34-24

Introduction

Targeted therapy is currently being studied extensively. For example, nanoparticles with a capacity to cross the blood-brain barrier are an attractive research target for potential treatments for neurological disorders [1]. One of the most common nanoparticles, which is used as a model, is nanodiamond (ND) of the smallest size (adamantane $C_{10}H_{16}$). The sequence of carbon atoms in its symmetrical structure (Fig. 1, *a*) is the same as in the crystal lattice of diamond, suggesting that this compound is an integral component of larger diamond-like compounds [2,3].

Simple chemical reactions modifying the ND surface, such as oxidation and amination, proceed in the course of non-covalent (adsorption) interaction of ND particles with various molecules [4], inducing the formation of surface carboxyl groups $-COOH$ or amino groups $-NH_2$, respectively [5,6]. Carboxyl groups (COOH) are the ones used most often in targeted delivery for adsorption immobilization of substances on the surface [7].

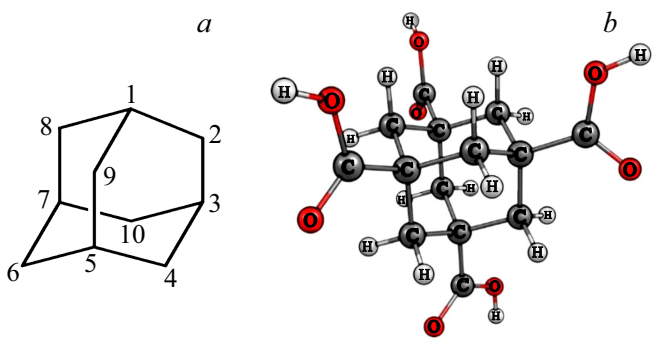

Figure 1. Structure of the carbon lattice of adamantane (*a*) and the adamantane-1, 3, 5, 7-tetracarboxylic acid (ATCA) molecule (*b*).

This interaction results in the formation of supramolecular complexes that retain the active substance on the ND surface via non-covalent interactions: ionic, ion-dipole, van der Waals, hydrophobic, and hydrogen bonds [8]. A considerable number of studies into the adsorption of various biologically active objects (e.g., proteins, enzymes, hormones, antibodies, drugs, toxins, and viruses) on the surface of ND have already been published [9]. The results of studies of cytotoxicity [10] and genotoxicity [11] of ND also suggest that the basic functions of cells, organs, and organisms are not impaired if ND is used in a reasonable concentration [10].

The authors of [12] state that adamantane-1, 3, 5, 7-tetracarboxylic acid (ATCA) [13] $C_{14}H_{16}O_8$ (Fig. 1, *b*), which is produced by substituting hydrogen atoms $-H$ at four main carbon atoms (1,3,5,7) in the adamantane structure with four carboxyl groups $-COOH$, provides for the most efficient and low-cost adsorption of substances onto the ND surface.

An in-depth study [14] characterizing the interaction of ATCA with the doxorubicin [15] and mitoxantrone [16] drugs has also been published. It was suggested there that a fairly strong supramolecular interaction based on hydrogen bonds may develop between these drugs and ATCA. This interaction may be regarded as one of the mechanisms of complexation for targeted delivery of a drug, retention of the drug in cells, and enhancement of its efficiency.

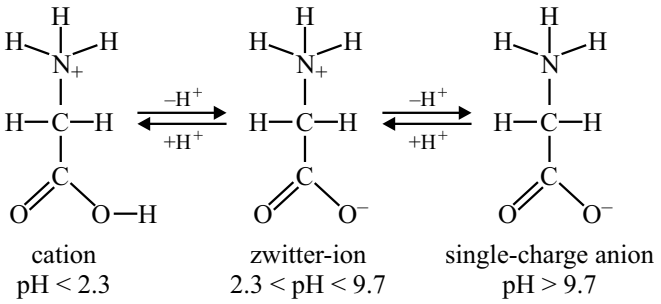

Figure 2. Ionic forms of glycine.

Glycine is an amino acid with the lowest molecular weight that consists of two hydrophilic groups ($-NH^+$, $-COO$) and one hydrophobic group ($-CH_2$); in addition, it has only one hydrogen atom as a side chain. It has been found earlier [17,18] that glycine is neutral in the gas phase, but its zwitterionic form is more stable than the neutral one in an aqueous solution and in the solid state in a neutral environment (pH 7). The process of transformation from the neutral form to the zwitterionic one is characterized [19] as a direct proton transfer between the carboxyl group ($-COO$) and the amino group ($I-NH^+$) (Fig. 2).

Glycine is used as a drug in neurology to reduce increased muscle tone, stimulate metabolism, and prevent cell death in the brain after a stroke [20]. In addition, it was confirmed in [21] that glycine in oral doses of 3–9 g improves sleep quality and does not cause serious side effects.

The aim of the present study is to examine spectral manifestations of the intermolecular interaction of the carboxylated ND–glycine complex with subsequent determination of the parameters of formed hydrogen bonds for evaluation of the degree of stability of this complex by analyzing its calculated structure and comparing its experimentally recorded and calculated IR spectra.

1. Experimental results

Experts working at LLC „Nauchnyi Tsentr RTA“ and involved with the development of new polymorphic modifications of pharmaceutical substances and their co-crystals unobtainable under normal synthesis conditions performed a number of experiments on the oxidation of ND, the positioning of glycine on the modified ND surface, and the examination of morphology of the resulting crystals.

Electron microscopical images of the samples were obtained using a LEO 1455 VP (Carl Zeiss, Germany) scanning electron microscope (SEM) with a Centarius detector. The samples to be imaged were deposited onto conductive double-sided tape and introduced into the microscope chamber, where the pressure was reduced to $10-5$ Torr.

The ND–glycine complex was also imaged with a JEM-2100F (JEOL, Japan) ultra-high-resolution transmission electron microscope (TEM), which has a point resolution of 2 Å and a lattice resolution of 1 Å.

The coherent scattering region (CSR) is denoted in red in Figs. 3, *a, b*, and its size in nanometers is indicated. Nanodiamond particles consist of a diamond core and a certain disturbed structure (shell) that is no longer a diamond one, but may be a different form of carbon in both sp^2 and sp^3- hybridization. It is this shell that is modified by $-COOH$ functional groups. The difference between carboxylated ND and pure ND is that the outer shell of carboxylated ND particles is more disturbed due to oxidation of their surface. This is evidenced by a comparison of the CSR sizes in Figs. 3, *a* and 3, *b*.

IR spectra of samples of carboxylated nanodiamonds, glycine, and their mixture are shown in Fig. 4. The spectra were recorded in pellets with KBr using an IR200 Thermonicolet (Thermo Scientific, United States) IR spectrometer with Fourier transform, which has a resolution of $2\,cm^{-1}$, at a temperature of 20°C.

A deeper analysis of the obtained experimental data requires calculation of the structure and IR spectra of the complex of carboxylated ND and glycine.

2. Computer modeling of IR spectra

Modeling of the structure and calculations of the frequencies of normal vibrations and the intensities of IR absorption bands of molecules and their complexes were carried out on the basis of density functional theory (DFT) [22] using the B3LYP functional and the 6-31G(d) basis set [23]. All molecular modeling procedures (including optimization of molecular structures and calculation of IR spectra) were performed in the Gaussian software package [24], which is used widely for molecular modeling in various fields of computational physics and chemistry, with the use of the Avogadro editor and visualizer of molecular structures [25] and proprietary IR spectra visualization software that plots an IR spectrum based on numerical values determined in Gaussian. Frequency scaling, which is used often by research groups around the world [26,27], was performed to obtain a closer agreement between measured and calculated spectra. The following scaling factors were used: 0.98 for the $0-2000\,cm^{-1}$ frequency range and 0.955 for the $2000-4000\,cm^{-1}$ frequency range.

The ATCA molecule, which is small in size but has the properties of large diamond structures, was chosen to be used as carboxylated ND for numerical modeling.. Using molecular modeling methods, we minimized energies and optimized the following structures: ATCA with glycine (ATCA_Glycine), ATCA with glycine and two water molecules (ATCA_Glycine_water), and ATCA with a glycine dimer (ATCA_2Glycine). The structures and IR spectra of the molecular complex of ATCA with one glycine molecule, one glycine molecule and two water molecules, and a glycine dimer were simulated. All calculations were carried out for a tem-

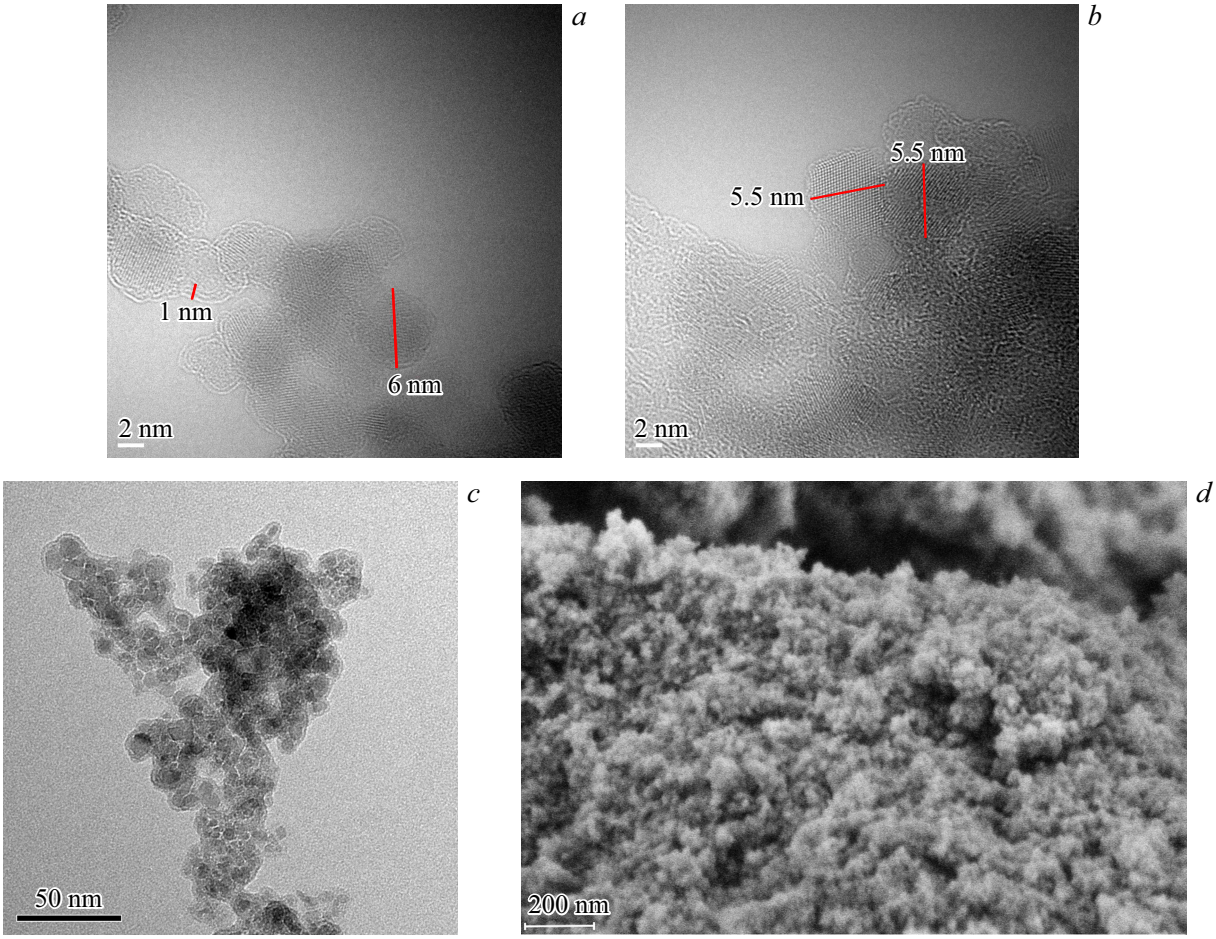

Figure 3. TEM (*a* — ND, the resolution is 2 nm; *b* — carboxylated ND, the resolution is 2 nm; *c* — carboxylated ND with glycine, the resolution is 50 nm) and SEM (*d* — carboxylated ND with glycine, the resolution is 200 nm) images of ND.

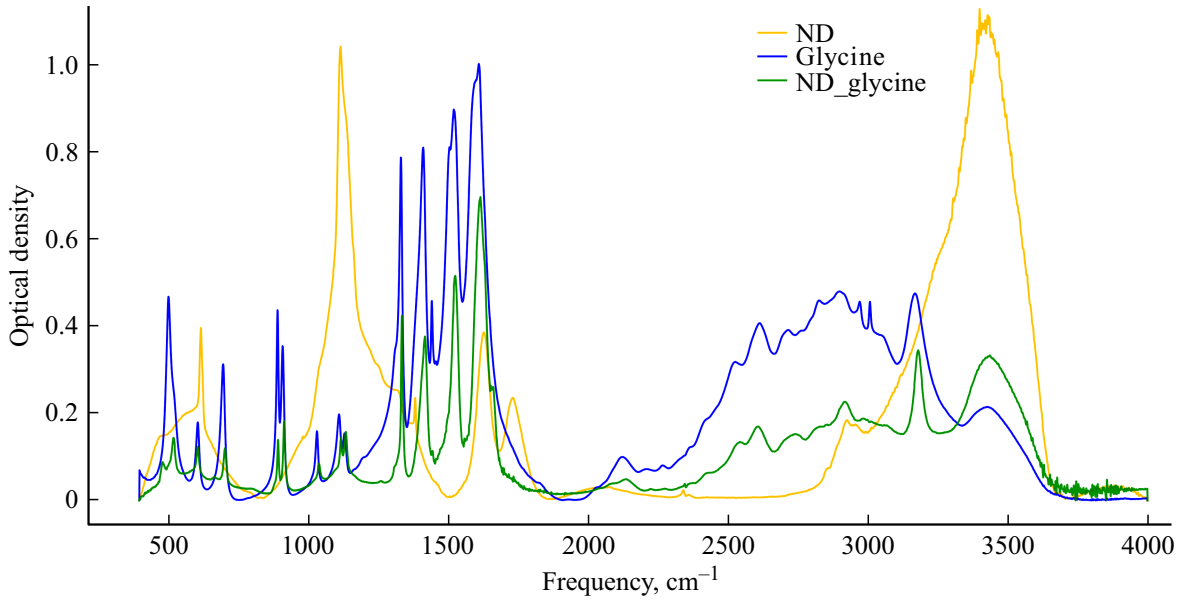

Figure 4. Experimental IR spectra (orange — carboxylated ND, blue — glycine, and green — carboxylated ND with glycine (ND_Glycine)).

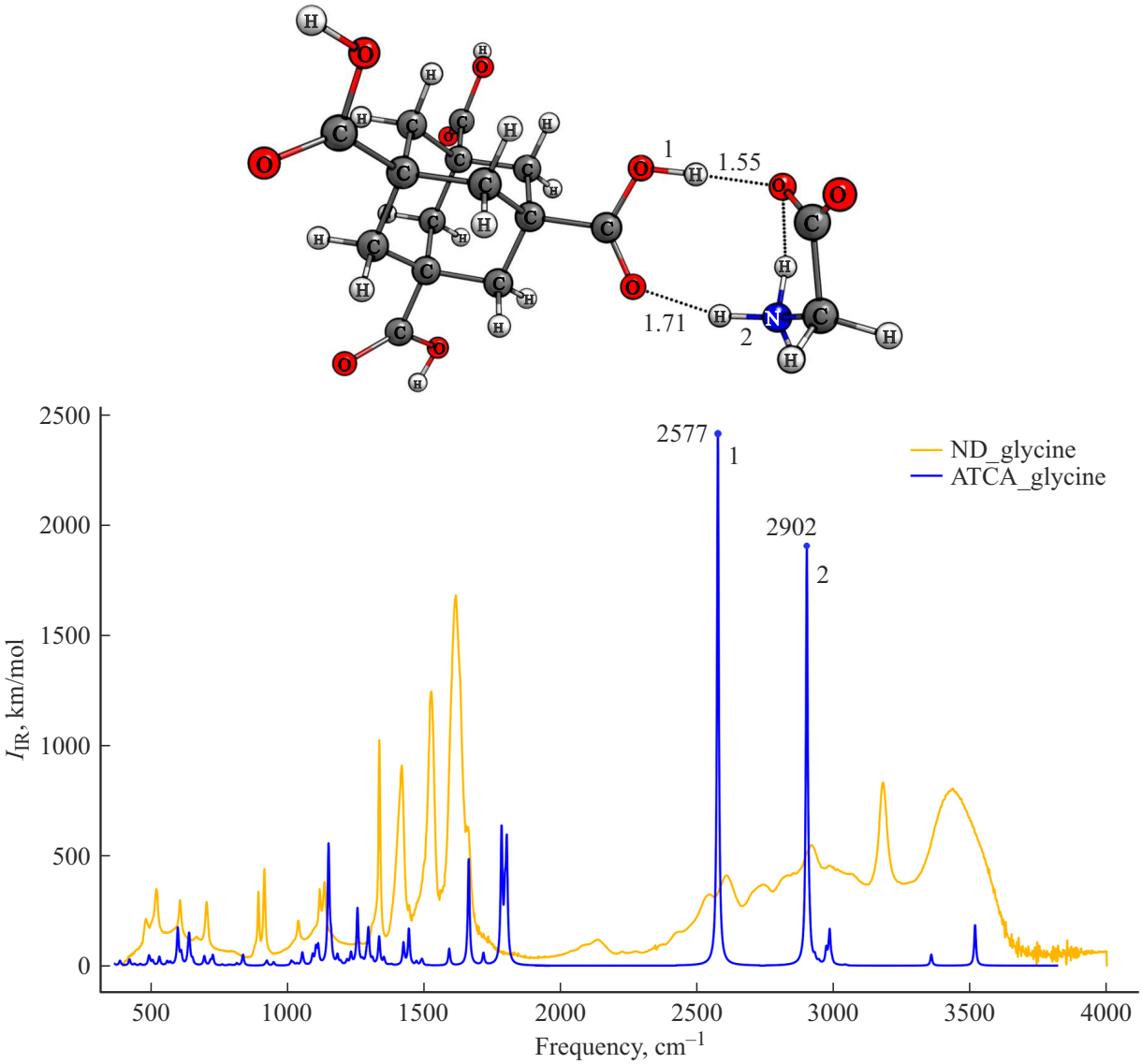

Figure 5. Calculated structure (top) and IR spectrum (bottom) of carboxylated ND with glycine (orange — experiment, blue — calculation). Numbers 1,2 mark the maxima of absorption bands corresponding to the vibrations of groups −OH (1) and −NH (2).

perature of 20°C that corresponds to the experimental conditions.

The strength of formed hydrogen bonds was assessed by the following parameters: the hydrogen bridge length, the frequency shift of valence vibrations of H-bonds in the IR spectrum of the molecular complex relative to the IR spectrum of individual molecules, and the bond energy.

The calculated structure and IR spectrum of the molecular complex of ATCA and glycine $(C_{14}H_{16}O_8)-(C_2H_5NO_2)$ are shown in Fig. 5. Dots denote the absorption band maxima of the calculated complex; frequencies corresponding to these absorption band maxima are indicated above the dots. Oxygen atoms (O) are marked in red, carbon atoms (C) are dark gray, nitrogen atoms (N) are blue, and hydrogen atoms (H) are light gray. Numbers 1,2 mark the maxima of absorption bands corresponding to the vibrations of groups −OH (1) and −NH (2). Figure 5 reveals fine agreement between the calculated and experimentally measured IR spectra in the high-frequency region. It can be seen that the absorption band maxima at frequencies of 2577 and 2902 cm^{-1} corresponding to bonds 1 and 2 are also present in the experimental spectrum, verifying the presence of individual glycine molecules in the composition of the studied substance.

It should be noted that the maximum of the absorption band in the 3400−3500 cm^{-1} region is characteristic of the IR spectrum of water molecules, which has been confirmed earlier [28] in the study of influence of single water molecules on the IR spectrum of modified glycine. Therefore, numerical modeling of the intermolecular interaction of ATCA and glycine with two water molecules $(C_{14}H_{16}O_8)-(C_2H_5NO_2)-(H_2O)_2$ (Fig. 6) was carried out

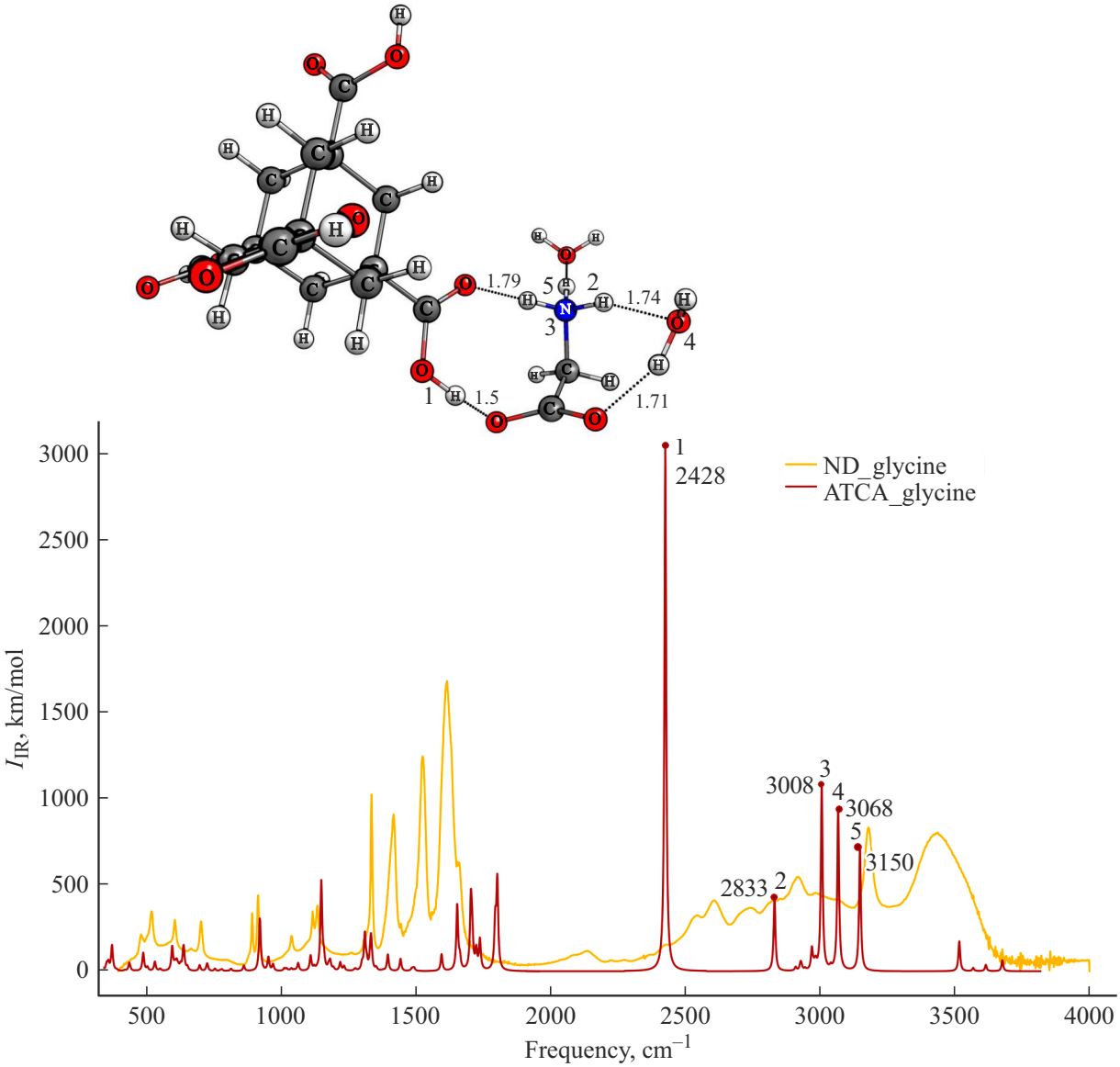

Figure 6. Calculated structure (top) and IR spectrum (bottom) of carboxylated ND with glycine and two water molecules (orange — experiment, brown — calculation). Numbers 1–5 mark the maxima of absorption bands corresponding to the vibrations of groups –OH (1,4) and –NH (2,3,5).

to reveal the influence of water. Numbers 1–5 mark the maxima of absorption bands corresponding to the vibrations of –OH (1,4) and –NH (2,3,5). It follows from the calculated IR spectrum that the number of hydrogen bonds (bonds 2,4,5) increased after the addition of two water molecules, thus increasing the overall stability of the complex. However, the absorption band maxima (2833, 3068, 3150 cm^{-1}) are not located in the characteristic frequency range corresponding to the valence vibration of the OH bond of water (3300–3650 cm^{-1}), implying that the effect of water molecules is insignificant in the experimental sample of ND with glycine.

The calculated structure and IR spectrum of the complex of ATCA and a glycine dimer $(C_{14}H_{16}O_8)-(C_2H_5NO_2)_2$ are shown in Fig. 7. Numbers 1–7 mark the maxima of absorption bands corresponding to the vibrations of groups –OH (1,4) and –NH (2,3,5,6,7). The results of calculations for this structure agree even better with the experiment. It is evident from a comparison with Fig. 5 that the number of hydrogen bonds between glycine and ATCA molecules has increased and bonds have formed between glycine molecules (e.g., bond 6). The absorption band maximum at a frequency of 3153 cm^{-1}, which corresponds to this bond, is seen clearly in the experimental spectrum, indicating the presence of dimers in the object under study and providing evidence of the influence of supramolecular complexation that increases the stability of the molecular ensemble.

Calculated parameters of hydrogen bonds of H-complexes ATCA−glycine and ATCA−glycine−water

Bond number	Bond type	H-bond length R, Å	Hydrogen bridge length R_B, Å	Frequency ν, cm^{-1}	Frequency shift $\Delta\nu, cm^{-1}$	Enthalpy -ΔH, kkal/mol	Intensity I_{IR}, km/mol
ATCA with glycine $E = -1429.420908$ a.u.							
1	O−H···O	1.55	2.58	2577	702	7.72	2412
2	N−H···O	1.71	2.73	2902	616	7.20	1876
ATCA with glycine and two water molecules $E = -1582.282806$ a.u.							
1	O−H···O	1.5	2.53	2428	1091	9.72	3048
2	N−H···O	1.74	2.74	2833	446	6.04	437
3	N−H···O	1.79	2.82	3008	270	4.55	1089
4	O−H···O	1.71	2.67	3068	450	6.07	955
5	N−H···O	1.85	2.89	3150	129	2.83	724
ATCA with a glycine dimer $E = -1713.860251$ a.u.							
1	O−H···O	1.59	2.55	2646	872	8.65	1988
2	N−H···O	1.7	2.72	2819	459	6.14	780
3	N−H···O	1.78	2.51	2898	380	5.53	232
4	O−H···O	1.67	2.64	2971	547	6.76	1739
5	N−H···O	1.96	2.52	3130	149	3.13	128
6	N−H···O	1.86	2.82	3153	125	2.77	635
7	N−H···O	1.97	2.85	3248	31	0	362

3. Assessment of hydrogen bonds

Let us now consider various complexation combinations and analyze the dynamics of changes in the parameters of the most significant hydrogen bonds. The strength of formed hydrogen bonds was assessed by the following parameters: the hydrogen bridge length and the frequency shift of valence vibrations of H-bonds in the IR spectrum of the molecular complex relative to the IR spectrum of individual molecules. The following bond parameters are listed in the table: type; R, Å– initial H-bond length; R_b, Å– N−H···O or O···H−O hydrogen bridge length (depending on the bond type); I_{IR}, km/mol — intensity of the absorption band maximum of the spectral line; and $\Delta\nu, \text{cm}^{-1}$ — frequency shift of valence vibrations of H-bonds in the IR spectrum of the molecular complex relative to the IR spectrum of individual molecules. This shift is needed to calculate bond energy ΔH, kcal/mol in accordance with the empirical Iogansen formula [29]:

$$-\Delta H = 0.3\sqrt{\Delta\nu - 40}. \quad (1)$$

The calculated parameters of hydrogen bonds for molecular complexes are presented in the table, where E is the energy of the molecular complex. The strength of formed hydrogen bonds was evaluated in accordance with the classification given in [8], where hydrogen bonds are considered strong if their energy is 14.34−28.65 kkal/mol and the hydrogen bridge length is 2.2−2.5 Å; bonds of a moderate strength have an energy of 3.82−14.43 kkal/mol and a hydrogen bridge length of 2.5−3.2 Å; and weak bonds have an energy lower than 2.87 kkal/mol and a hydrogen bridge length of 3.2−4.0 Å.

The value of $\Delta\nu$ was calculated based on the frequencies of valence vibrations of H-bonds in the IR spectrum of individual glycine [28] and ATCA [14] molecules with the following scaling factors: ν_{glycine} N−H = 3279 cm^{-1} and ν_{ATKK} O−H = 3518 cm^{-1}.

Let us consider different types of complexation of glycine with ATCA. It follows from the table that two hydrogen bonds O−H···O are formed when the glycine molecule interacts with ATCA. They may be classified as moderate-strength bonds, since they have frequency shifts of 702 and 616 cm^{-1} and intensities of 342 and 581 kkal/mol, respectively.

The complex of ATCA, glycine, and two water molecules is shown in Fig. 6. Bonds number 2 and 5 (N−H···O) and bond number 4 (O−H···O) form between glycine and water. Two of them (namely, bonds 2 and 4) may be classified as moderate-strength bonds with 6.04 and 6.07 kkal/mol. Bond number 5 has a frequency shift of 129 cm^{-1} and a hydrogen bond length of 1.85 Å, which makes it a weak bond. Bonds 1 (O−H···O) and 3 (N−H···O) may be classified as moderate-strength ones, since they have frequency shifts of 1091 and 270 cm^{-1} and intensities of 3048 and 1089 kkal/mol, respectively.

When a glycine dimer is added to ATCA, seven hydrogen bonds form in the complex (Fig. 7). Two glycine molecules interact with each other through hydrogen bond 6, which

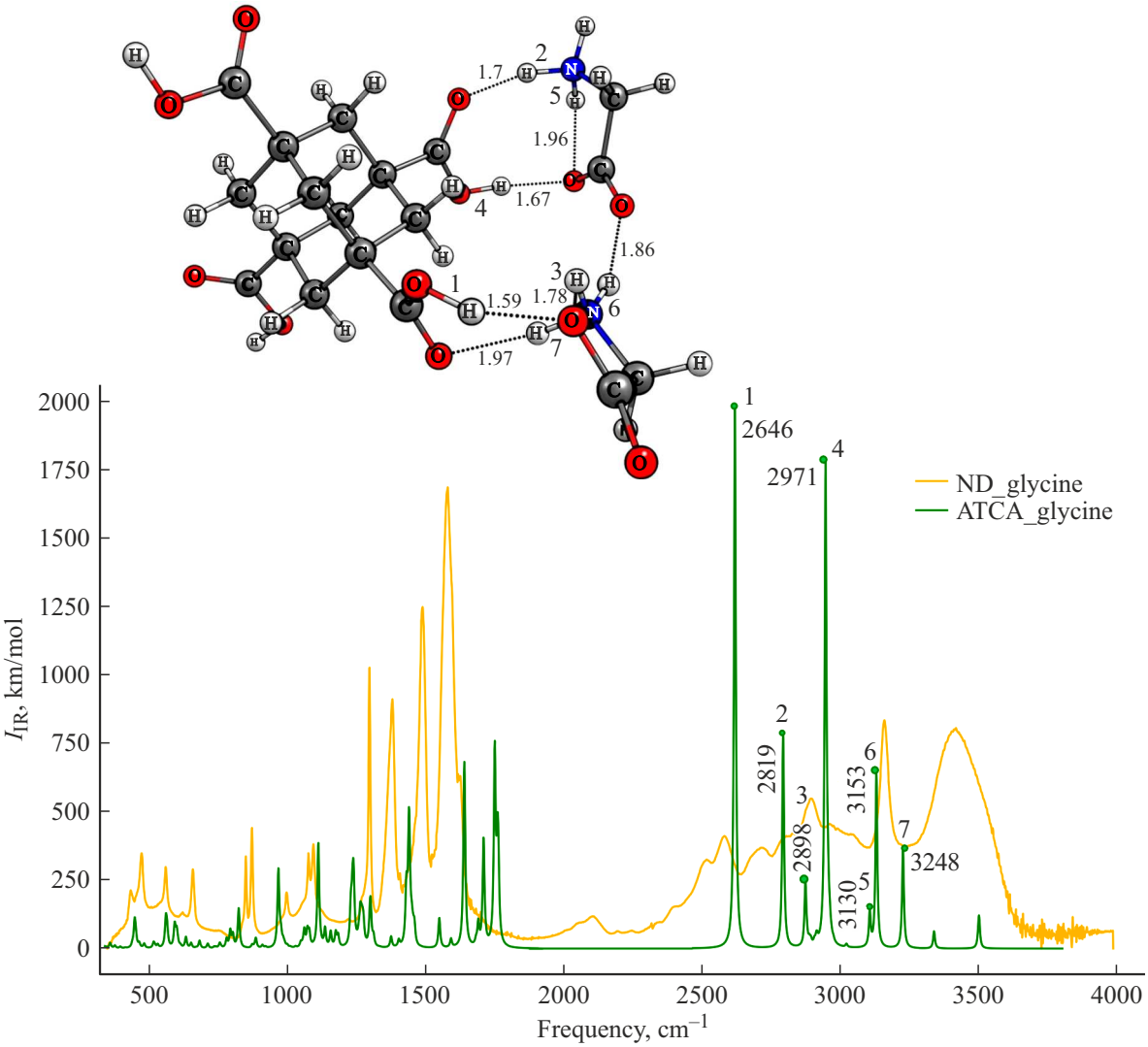

Figure 7. Calculated structure (top) and IR spectrum (bottom) of carboxylated ND with a glycine dimer (orange — experiment, green — calculation). Numbers 1–7 mark the maxima of absorption bands corresponding to the vibrations of groups –OH (1,4) and –NH (2,3,5,6,7).

is the weakest of all stable bonds in this complex, since its energy is 2.76 kal/mol. Two bonds of the O–H···O type, which formed between ATCA and glycines, turned out to be close to the upper boundary for moderate bonds. Their frequency shift was 872 and 547 cm^{-1}, and the intensity was 1988 and 1739 kkal/mol. Bonds number 2 and 3 are of the N–H···O type and may be classified as moderate ones with energies of 6.14 and 5.53 kkal/mol, respectively. Bond number 7 may be called insufficiently stable, since it has a long hydrogen bridge (longer than 1.97 Å).

4. Conclusion

Spectral manifestations of the intermolecular interaction of carboxylated ND with glycine, which reveals itself in the form of hydrogen bonding in a two-component mixture, were studied. It was found that carboxylated ND has the capacity to interact efficiently with glycine through the formation of stable hydrogen bonds. Hydrogen bonds forming between carboxylated ND and glycine help maintain the structural stability of a complex and ensure the stability of interaction under delivery conditions.

Thus, the present study offers new insight into the interaction of carboxylated ND with glycine and is an important step in the development of new drug delivery methods. These results contribute to expanding our knowledge of nanotechnology in medicine and open prospects for further research and development in the field of innovative pharmacology.

Conflict of interest

The authors declare that they have no conflict of interest.

References

[1] R.G. Mendes, P.S. Wróbel, A. Bachmatiuk, J. Sun, T. Gemming, Z. Liu, M.H. Rümmeli. J. Mater. Chem. B, **1** (4), 401–428 (2013). DOI: 10.1039/c2tb00085g

[2] E.I. Bagrii. *Adamantany: Poluchenie, svoistva, primenenie* (Nauka, M., 1989) (in Russian).

[3] G.A. Mansoori. Adv. Chem. Phys., **136**, 207–258 (2007).

[4] A.Ya. Vul, O.A. Shenderova. *Detonation Nanodiamonds: Science and Applications* (CRC Press, Boca Raton, Florida, USA, 2014).

[5] A. Krueger, D. Lang. Adv. Funct. Mater., **22** (5), 890–906 (2012). DOI: 10.1002/adfm.201102670

[6] D.H. Jariwala, D. Patel, S. Wairkar. Mater. Sci. Engin. C, **113**, 110996 (2020). DOI: 10.1016/j.msec.2020.110996

[7] D.G. Lim, K.H. Kim, E. Kang, S.H. Lim, J. Ricci, S.K. Sung, M.T. Kwon, S.H. Jeong. Int. J. Nanomedicine, **11**, 2381–2395 (2016). DOI: 10.2147/IJN.S104859

[8] J.W. Steed, J.L. Atwood, *Supramolecular Chemistry* (Wiley, Chichester, 2000).

[9] J.M. Say, C. van Vreden, D.J. Reilly, L.J. Brown, J.R. Rabeau, N.J.C. King. Biophys. Rev., **3** (4), 171–184 (2011). DOI: 10.1007/s12551-011-0056-5

[10] K. Turcheniuk, V.N. Mochalin. Nanotechnology, **28** (25), 252001 (2017). DOI: 10.1088/1361-6528/aa6ae4

[11] Y. Xing, W. Xiong, L. Zhu, E. Osawa, S. Hussin, L. Dai. ACS Nano, **5** (3), 2376–2384 (2011). DOI: 10.1021/nn200279k

[12] A.N. Bokarev, I.L. Plastun. *Mezhmolekulyarnoe vzaimodeistvie almazopodobnykh nanochastits s lekarstvennymi preparatami i biomolekulami* (EBS ASV: Sarat. Gos. Tekh. Univ., Saratov, 2020) (in Russian).

[13] O. Ermer. J. Am. Chem. Soc., **110** (12), 3747–3754 (1988). DOI: 10.1021/ja00220a005

[14] I.L. Plastun, A.N. Bokarev, A.A. Zakharov, A.A. Naumov. Fullerenes Nanotubes and Carbon Nanostructures, **28** (3), 183–190 (2020). DOI: 10.1080/1536383X.2019.1686618

[15] A.D. Salaam, P.T.J. Hwang, A. Poonawalla, H.N. Green, H-W. Jun, D. Dean. Nanotechnology, **25** (42), 425103 (2014). DOI: 10.1088/0957-4484/25/42/425103

[16] T.B. Toh, D.-K. Lee, W. Hou, L.N. Abdullah, J. Nguyen, D. Ho, E.K.-H. Chow. Molecular Pharmaceutics, **11** (8), 2683–2691 (2014). DOI: 10.1021/mp5001108

[17] G. Albrecht, R. Corey. J. Am. Chem. Soc., **61**, 1087–1103 (1939). DOI: 10.1021/ja01874a028

[18] Y. Ding, K.J. Krogh-Jespersen. J. Comput. Chem., **17**, 338–349 (1996). DOI: 10.1002/(SICI)1096-987X(199602)17:3%3C338::AID-JCC8%3E3.0.CO;2-W

[19] K. Leung, S. Rempe. J. Chem. Phys., **122** (18), 184506 (2005). DOI: 10.1063/1.1885445

[20] O.A. Gromova, I.Yu. Torshin, E.I. Gusev, A.A. Nikonov, O.A. Limanova. Trudny Patsient, **8** (4), 25–31 (2010) (in Russian).

[21] M. Bannai, N. Kawai. J. Pharm. Sci., **118** (2), 145–148 (2012). DOI: 10.1254/jphs.11r04fm

[22] W. Kohn. Rev. Mod. Phys., **71** (5), 1253–1265 (1999). DOI: 10.1103/RevModPhys.71.1253.

[23] A.D. Becke. J. Chem. Phys., **98** (7), 5648–5652 (1993). DOI: 10.1063/1.464913

[24] M.J. Frisch, G.W. Trucks, H.B. Schlegel, G.E. Scuseria, M.A. Robb, J.R. Cheeseman, J.A. Montgomery, Jr.T. Vreven, K.N. Kudin, J.C. Burant, J.M. Millam, S.S. Iyengar, J. Tomasi, V. Barone, B. Mennucci, M. Cossi, G. Scalmani, N. Rega, G.A. Petersson, H. Nakatsuji, M. Hada, M. Ehara, K. Toyota, R. Fukuda, J. Hasegawa, M. Ishida, T. Nakajima, Y. Honda, O. Kitao, H. Nakai, M. Klene, X. Li, J.E. Knox, H.P. Hratchian, J.B. Cross, C. Adamo, J. Jaramillo, R. Gomperts, R.E. Stratmann, O. Yazyev, A.J. Austin, R. Cammi, C. Pomelli, J.W. Ochterski, P.Y. Ayala, K. Morokuma, G.A. Voth, P. Salvador, J.J. Dannenberg, V.G. Zakrzewski, S. Dapprich, A.D. Daniels, M.C. Strain, O. Farkas, D.K. Malick, A.D. Rabuck, K. Raghavachari, J.B. Foresman, J.V. Ortiz, Q. Cui, A.G. Baboul, S. Clifford, J. Cioslowski, B.B. Stefanov, G. Liu, A. Liashenko, P. Piskorz, I. Komaromi, R.L. Martin, D.J. Fox, T. Keith, M.A. Al-Laham, C.Y. Peng, A. Nanayakkara, M. Challacombe, P.M.W. Gill, B. Johnson, W. Chen, W. Wong, C. Gonzalez, J.A. Pople. *Gaussian03, Revision B.03* (Gaussian, Inc., Pittsburgh PA, 2003), p. 302

[25] Avogadro–Free cross-platform molecular editor. [Electronic source]. URL https://avogadro.cc/

[26] H. Yoshida, A. Ehara, H. Matsuura. Chem. Phys. Lett., **325** (4), 477–483 (2000). DOI: 10.1016/S0009-2614(00)00680-1

[27] H. Yoshida, K. Takeda, J. Okamura, A. Ehara, H. Matsuura. J. Phys. Chem. A., **106** (14), 3580–3586 (2002). DOI: 10.1021/jp013084m

[28] I.L. Plastun, P.A. Zhulidin, P.D. Filin, R.Yu. Yakovlev. Opt. Spectrosc., **131** (6), 787–794 (2023). DOI: 10.21883/OS.2023.06.55918.118-23

[29] A.V. Iogansen. *Vodorodnaya svyaz'* (Nauka, M., 1981) (in Russian).

Translated by D.Safin